Journal of Hazardous Materials 172 (2009) 729–738

Contents lists available at ScienceDirect

Journal of Hazardous Materials

journal homepage: www.elsevier.com/locate/jhazmat

Biosorption of Ga-67 radionuclides from aqueous solutions onto waste pomace of an olive oil factory

Hayrettin Eroglu[a,*], Sinan Yapici[b], Cigdem Nuhoglu[c], Erhan Varoglu[a]

[a] Department of Nuclear Medicine, Ataturk University, 25240 Erzurum, Turkey
[b] Department of Chemical Engineering, Ataturk University, 25240 Erzurum, Turkey
[c] Department of Physics, Faculty of Science, Ataturk University, 25240 Erzurum, Turkey

ARTICLE INFO

Article history:
Received 21 April 2009
Received in revised form 12 June 2009
Accepted 14 July 2009
Available online 22 July 2009

Keywords:
Gallium-67
Biosorption
Radionuclide
Radioactivity
Heavy metal

ABSTRACT

The aim of this research was to test the removal of Ga-67 radionuclides from aqueous solutions by biosorption onto waste pomace of an olive oil factory (WPOOF). Batch adsorption studies were performed in order to investigate the temperature, the initial pH of the solution, the stirring speed, the biosorbent dose, and the nominal particle size of the biosorbent in the experimental work. The most effective parameter was found to be the initial pH. A high biosorption yield of 98 was obtained. The equilibrium values were fitted to the isotherm models. The values of ΔG and ΔH were calculated to be negative. The adsorption kinetics calculations showed that the kinetics of the biosorption process fitted well to the pseudo-second order rate model.

1. Introduction

Global warming and population growth have increased the need for clean water. The increased use of nuclear materials brings the need to avoid their harmful effects on the environment. There are various ways of removing radionuclides, which are ionized species, from radioactive waste water, such as reverse osmosis, ion exchange, precipitation, and coagulation. However, these methods are quite expensive and are not so efficient in the case where the waste contains radionuclides in low concentrations. Therefore, after the treatment with one of the above methods, the waste still contains poisonous materials [1]. The use of biosorbents for removing radionuclides has some advantages over the abovementioned methods and has been becoming more important [2].

In nuclear medicine, diagnoses and treatments are done by using radioactive materials. The discharge of radionuclides from patients or of the unused radioactive substances into the environment can cause serious radioactive problems and can be deadly. In addition to radioactive contamination, it causes heavy metal contamination and poisoning because radionuclides convert to stable heavy metal ions when they decay to steady states. When they mix with underground water, their harmful effects become unavoidable [3].

The precautions taken to remove harmful effects of these radioactive materials used in nuclear medicine are neither practical nor suitable. Especially, the method of keeping them in lead covered rooms is a slow, expensive, and time-consuming method since it requires a considerable amount of time for radioactive materials to become stable. It is preferred to remove harmful materials by using different techniques. Medine, in a study performed in 2003, preferred to remove radioactive materials by using ion converters and used Amberlit ion converter resins to remove iodine-131 used in nuclear medicine [4]. Koshima studied the removal of thallium(III), gallium(III), gold(III), and ferric(III) ions from the hydrochloride solution by using AmberliteXAD ve Chelex100 resins [5]. Taner studied the adsorption of Cr-51 used in nuclear medicine by employing the water plants of *Eichhornia crassipes*, *Pistia* sp., *Nymphaea alba*, *Mentha aquatica*, *Euphorbia* sp., and *Lemna minor* as biosorbents [6]. Activated carbon was also used for removing some radionuclides from aqueous media, such as uranium [7] and iodine [8]. Osmanoğlu studied the adsorption of radionuclides (^{137}Cs, ^{60}Co, ^{90}Sr and ^{110m}Ag) on zeolites, and Clinoptilolite were shown to have a high selectivity for ^{137}Cs and ^{110m}Ag as sorbent [9].

Gallium citrate is used for the purpose of the visualisation in nuclear medicine and is converted to zinc after decaying [10,11].

$$^{67}\mathrm{Ga} \rightarrow {}^{67}\mathrm{Zn} + \gamma^{-2}\,93\,\mathrm{keV}\,(\%38) + \gamma^{-3}\,185\,\mathrm{keV}\,(\%24) + \gamma^{-5}\,300\,\mathrm{keV}\,(\%16) + \gamma^{-6}\,394\,\mathrm{keV} \quad (t_{1/2} = 78.25\,\mathrm{h}) \tag{1}$$

The removal of Ga-67 from waste water is important due to both its radioactivity and conversion to a heavy metal, Zn-67, after losing its radioactivity. The aim of this work is to investigate the adsorption

* Corresponding author. Tel.: +90 442 231 6653; fax: +90 442 231 2766.
E-mail address: heroglu@atauni.edu.tr (H. Eroglu).

0304-3894/$ – see front matter © 2009 Elsevier B.V. All rights reserved.
doi:10.1016/j.jhazmat.2009.07.054

Nomenclature

B_r	the resonance magnetic field
C	concentration of adsorbate in the solution at equilibrium ($mg\,L^{-1}$)
D	diffusion coefficient (cm^2/s)
E	adsorption free energy (J/mol)
E_a	activation energy (J/mol)
G	Gibbs free energy (J/mol)
H	enthalpy (J/mol)
h	Planck constant (J s)
K	constant related to adsorption capacity ($L\,g^{-1}$)
k	kinetic rate constant
k_D	the distribution coefficient
K_1	constant related to adsorption energy ($mol^2\,kJ^{-2}$)
k_i	intraparticular diffusion coefficient ($mg/g\,s^{0.5}$)
n	constant related to adsorption intensity
q	adsorbed amount per amount adsorbent at equilibrium ($mg\,g^{-1}$)
r	adsorbent particle radius (cm)
R	ideal gas constant ($8.314\,J\,K^{-1}\,mol^{-1}$)
R	regression coefficient
r_o	nominal particle radius of adsorbent (cm)
S	entropy ($J\,mol^{-1}\,K^{-1}$)
T	absolute temperature (K)
t	time (min)

Subscripts

1/2	half-life time
ads	adsorbed
e	equilibrium
m	theoretical capacity
o	initial value
t	any time
thr	theoretical

Greek letters

Δ	change
β	the Bohr magnetron
ε	Polany potential
μ	micro
ν	the microwave frequency

of the radioactive ions of Ga-67 from waste water by using the solid waste from olive oil plants as biosorbents and to study the effect of some experimental parameters on the adsorption yield.

2. Materials and methods

2.1. Adsorbent

The olive fruits of *Olea europea sativa* are used to obtain olive oil by various physical methods. Olive pomace and black liqueur are obtained as side products. Prina is a residue of olive pomace derived from the olive oil process, and approximately 60–70 kg of dry prina with no oil are obtained from 100 kg of pomace [12].

In the present study, prina was obtained from the olive oil plants around Manisa in the Aegean region of Turkey. Prina was first washed by distilled water a few times until the filtered water became clear and then dried at room temperature. Dried prina was ground with a grinder and then sieved to obtain desired nominal particle size fractions. The density, nominal particle size, and BET surface area of prina were determined to be $0.1510\,g/cm^3$, 0.15–0.71 mm, and $0.7902\,m^2/g$, respectively.

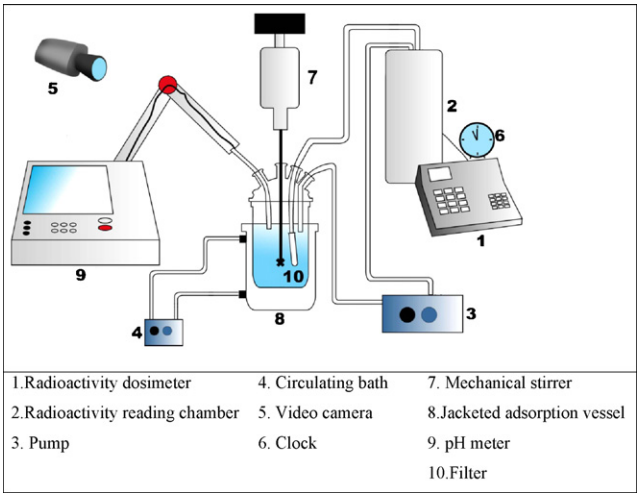

Fig. 1. Experimental system.

2.2. Experimental system

The experimental system is shown in Fig. 1. A 1000 mL jacketed glass vessel was employed as the adsorption medium. A mechanical mixer was used to stir the content of the vessel during the biosorption process. A circulating bath with a thermostat was employed to keep the adsorption medium at constant temperature. A master flex pump circulated the aqueous solution through the radiation dosimeter to automatically measure the radioactivity of the solution. The circulation of biosorbent particles together with the solution was avoided by using a suitable filter, which does not adsorb the radioactive substance, just at the outlet of the solution from the vessel. The experimental readings were recorded by a video camera to minimize the involvement of the researcher with the radioactive medium.

The radioactivity was performed measured in the unit of Curie (Ci) by using a radioactivity dose calibrator (Biodex, Atomlab 200 model dose calibrator) used in nuclear medicine applications. Before carrying out the experiment, all the necessary information for the calculation of concentration and radioactivity was provided from the manufacturer. The radioactivity per mass is called specific activity, which is 10 mCi/μg for Ga-67. By using the specific activity value, the amount of radionuclide in gram corresponding to the radioactivity in Ci was determined. The average specific activity of Ga-67 was 10 mCi/μg.

The electrical potential at the surface of a particle is called zeta potential. It is determined by measuring the velocity of particles in an electric field. The results are given in Table 1; the table shows that increasing pH increases the zeta potential of olive pomace particles. At neutral conditions, the surface charge has a negative value of −41.5 with increasing pH, the concentration of OH^- increases. This causes an increase of the negative charge of the surface by neutralising the positive groups on the surface. When pH of the solution is reduced, the increasing H^+ ions decreases surface negative charge by affecting the negative groups on the surface.

The experimental parameters were chosen to be the pH, stirring speed, biosorbent dose, nominal particle size, and temperature. When the effect of one parameter on the biosorption was investigated, the values of the other parameters were kept constant at

Table 1
Zeta potential of olive pomace at different pH values.

pH	4.0	6.0	7.0	8.0	10.0
Zeta potential (mV)	−36.5	−38.6	−41.5	−54.1	−54.7

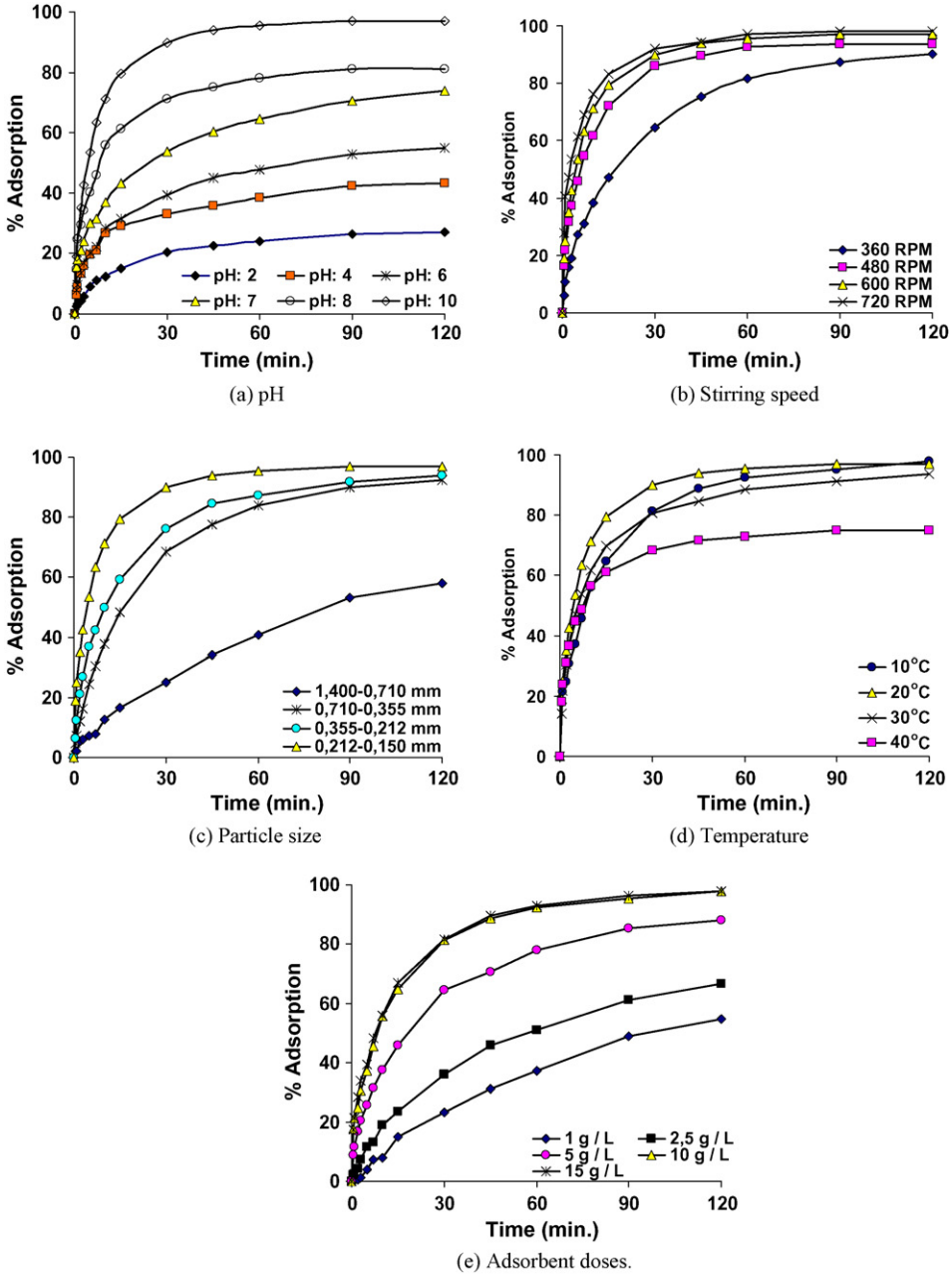

Fig. 2. Effect of experimental parameters on biosorption. (a) pH; (b) stirring speed; (c) particle size; (d) temperature; (d) adsorbent doses.

10.0 for the pH, 0.150–0.212 mm for the particle size, 10 g/L for the adsorbent dose, 20 °C for temperature, and 600 rpm for the stirring speed.

2.3. Preparation of radioactive solution

The radionuclide solution of Ga-67 was prepared by taking into consideration the specific radioactivity and calibration date of the sample and by using a dose calibrator. A given amount of the biosorbent was added to the solution whose pH level, temperature, and stirring speed were previously adjusted. The radionuclide concentration of the solution was determined by taking the approximate average value of the aqueous waste excreted by patients. It was not safe to prepare solutions in higher concentration values due to the difficulties in working conditions and the harmful effect on the researcher caused by high radiation.

2.4. The FTIR and EPR analyses

The FTIR spectra were obtained and transferred to Microsoft Excel using the PerkinElmer Spectrum One model FTIR spectrometer.

The EPR spectra were obtained from an x-band EPR spectrometer at 9.53 GHz using the Varian E104 model EPR spectrometer with modulation of magnetic field of 100 kHz. The microwave frequency was recorded. To avoid microwave saturation of resonance absorption curves, the natural and chromium loading EPR signals of the biomasses were also observed with attention of 23 dB.

3. Results and discussion

The removal of Ga-67 from the aqueous solution was investigated in a batch process. The adsorption values in 120 min were

used in the calculation since equilibrium was reached in 120 min. The effects of the chosen parameters on the adsorption process of Ga-67 by prina were investigated to determine the process conditions in a batch system. The results are shown in Fig. 2. The equilibrium condition for the process was reached in 120 min; therefore, the isotherm calculations were performed by using the biosorption data for a biosorption period of 120 min.

3.1. Effect of the pH

The effect of the pH on the adsorption process was investigated for pH values of 2.0, 4.0, 6.0, 7.0, 8.0, and 10.0. The change of the adsorbed percentage of Ga-67 with the pH is given in Fig. 2(a) as a function of the adsorption period. As seen from the figure, increasing the pH increased the adsorption of Ga-67 up to pH 10.0. At pH 10.0, approximately 97% of the initial amount of Ga-67 was adsorbed after 120 min while only about 27% of Ga-67 was removed at pH 2.0 in the same period. This increase with the pH can be explained by the rise in the negative value of prina's surface charge, which is called zeta potential, with pH increases as shown in Table 1. At pH 10.0, the surface charge has a negative value of −54.7. Increasing the pH increases the concentration of OH^-; these OH^- ions increase the negative charge of the surface by neutralising the positive groups on the surface. In the case of a pH decrease, the increasing H^+ ions decrease the surface negative charge by affecting the negative groups on the surface. Since Ga-67 ion has an electrical charge of +3, increasing the surface negative charge increases the biosorption yield due to the effect of electrical forces.

3.2. Effect of the stirring speed

The effect of the stirring speed on the biosorption of Ga-67 on prina was studied for the stirring speed values of 360, 480, 600, and 720 rpm. The results are given in Fig. 2(b) for different stirring speed values as a function of time. Increasing the stirring speed resulted in a small increase in the biosorption yield. In 120 min of the biosorption period, the biosorption percentage was 98% at 720 rpm, and the yield decreased to 90.3% when the stirring speed was reduced to 320 rpm. This small change can be attributed to the decrease in the liquid film thickness around the biosorbent particle with the increase in the stirring speed; it can cause a slight increase in the arrival rate of Ga-67 ions to the surface of the biosorbent. This behaviour indicates that the process is not controlled by the mass transfer of Ga-67 through the film layer around the particle.

3.3. Effect of the adsorbent particle size

To observe the effect of the nominal biosorbent particle size on the biosorption, the nominal particle sizes were chosen to be 1.40–0.71, 0.71–0.355, 0.355–0.212, and 0.212–0.150 mm. The change of the biosorption percentage with the nominal particle size is presented in Fig. 2(c) in the plot of the biosorption percentage as a function of the period. The figure shows that the change in the particle size has an important effect on the process. Decreasing the particle size increases the biosorption rate; for example, for the biosorption process of 120 min, 97% of the initial amount of Ga-67 was removed when the particle size was 0.150–0.212 mm, and the yield was reduced to 57.9% when the nominal particle size was 0.710–1.400 mm. This change can be attributed to the increase in the outer surface area per weight of the solid and the decrease in the nominal transfer distance into the particle with the decrease of the particle size. This behaviour with the change in the particle size shows that the diffusion of Ga-67 through the pores in the biosorbent may be an important step in controlling the rate of the biosorption process.

3.4. Effect of temperature

The effect of temperature on the adsorption was investigated for the temperatures of 10, 20, 30, and 40 °C. The plot of the adsorption percentage against time is given in Fig. 2(d) for different temperatures. Increasing the temperature decreased the adsorption percentage; the highest removal percentage was obtained at 10 °C. For the adsorption period of 120 min, approximately 98% of the initial amount of Ga-67 was removed at 10 °C while 75% was adsorbed at 40 °C. The effect of temperature on the process is slightly more pronounced than those of the stirring speed and particle size and less pronounced than that of the pH. This behaviour indicates that the adsorption process has a physical and exothermic character.

3.5. Effect of the adsorbent dose

The effect of the adsorbent dose on the biosorption was studied by carrying out some experiments at different adsorbent doses of 1.0, 2.5, 5.0, 10.0, and 15.0 g solid/L solutions while the values of the other parameters were kept at 10.0 pH, 0.150–0.212 mm particle size, 600 rpm stirring speed, and 10 °C temperature. The results are shown in Fig. 2(e). As seen from this figure, the biosorption percentage increased with increasing the adsorbent dose, and the maximum yield was obtained at 15 g/L. However, the increases were smaller with increasing values of the dose. The removal percentage was 98 for 15 g/L and 40.5 for 1 g/L for an adsorption period of 120 min. The increase in the adsorption with the increase in the adsorbent dose can be explained by the increase of the available adsorption area for a constant initial value of the Ga-67 concentration.

3.6. Adsorption isotherms

The adsorption isotherm, which is also called the equilibrium line, represents the relation between the adsorbed amount per mass of the adsorbent and the non-adsorbed amount per volume of fluid at equilibrium for a given temperature. The isotherms exhibit various behaviours depending upon the characteristics of the adsorbent and adsorbate, and the adsorption mechanism. In the present work, the equilibrium lines were obtained by changing the biosorbent dose instead of changing the initial concentration of Ga-67 since increasing the concentration of the radionuclide is not safe due to the high radioactivity that causes harmful effect on the environment and workers. The adsorption isotherms were studied by using the data given in Fig. 2(e), and the isotherms are presented graphically in Fig. 3. The isotherm models were tested to find which models represent the equilibrium line in Fig. 3. The models, which give meaningful results, are shown below. Some bends are noticeable in Fig. 3. When the graph is analyzed, it is seen that the

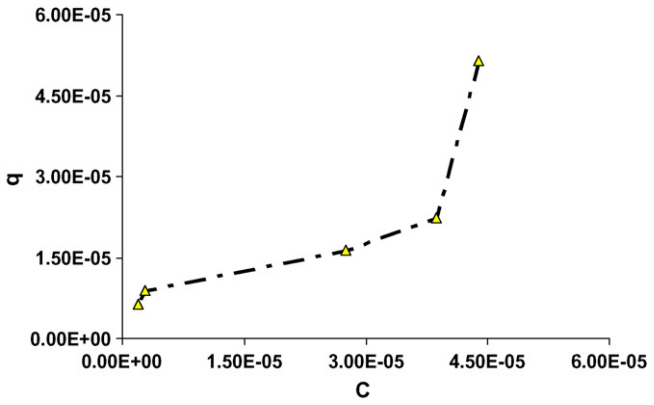

Fig. 3. Adsorption isotherm.

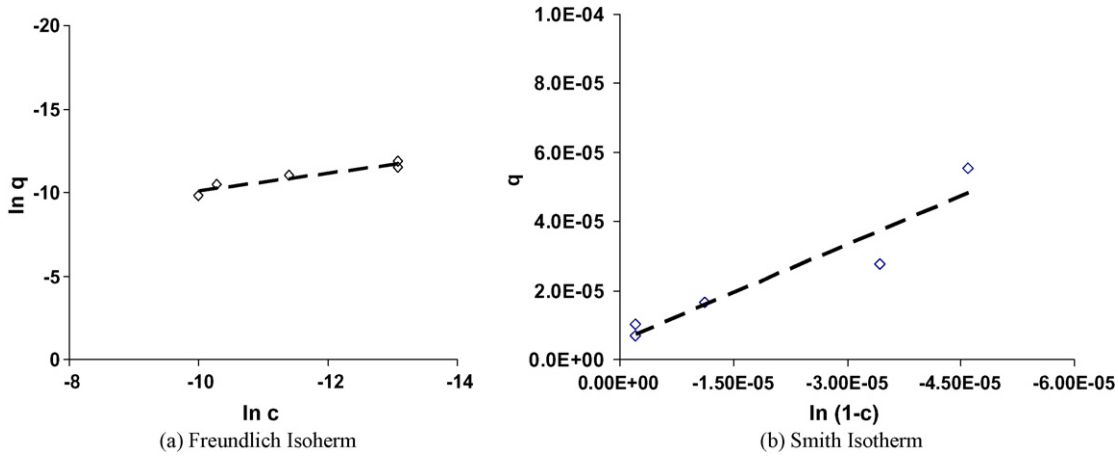

Fig. 4. (a) Fit of data to Freundlich model and (b) fit of data to Smith model.

bend point of the isotherm can be attributed to the completion of the first adsorbed layer. Consequently, when the concentration increases, the number of levels increases unlimitedly: that is, additional adsorptions occur with the proceeding biosorption [13,14]. Therefore, it can be expressed that the process is multilayered adsorption. Other isotherm models also support multilayered adsorption, and the data for those are given in Fig. 4.

The statistical analysis showed that the isotherm models of Freundlich, Halsey, Henderson, D–R and Smith fitted well the isotherm data for the present work, and the Langmuir model did not. The fit of the data to the Freundlich, Halsey, Henderson, D–R, and Smith isotherms indicates that the active sites on the biosorbent surface have a heterogeneous structure that consists of adsorption sites of various species; it also indicates that the adsorption is multilayered [15–18]. The model equations, the values of the constants in these equations, and the squares of the regression coefficients of the above models are given in Table 2.

In the Freundlich isotherm, K having a small value and n being greater than one strengthen the conclusion that multilayered adsorption occurs. In Freundlich, Halsey, Henderson, D–R, and Smith isotherms, a high regression coefficient also shows that multilayered adsorption occurs. Furthermore, it indicates the possibility of the existence of heteroporosis.

In the D–R isotherm, the E value gives information about the biosorption mechanism regarding if it is physical adsorption or not. The numerical values of E calculated from the Eq. (8) is 11.18 kJ mol^{-1}. The mean free energy of the biosorption of Ga-67 on olive pomace, E, characterises a physical adsorption and the predominance of van der Waals forces [19].

Langmuir's isotherm model was also analyzed, but it was not commented on since the regression coefficient was found to be low. However, it is meaningful that the data do not agree with this model because this model is used to explain single-layered adsorption.

As a result, it can be concluded that the adsorption process has a multilayered character, and the adsorption surface is not uniform and possibly has a heterogeneous structure.

Table 2
Model constants and regression coefficients of isotherm models.

Isotherms	Model equation	Equation no.	Value	R^2
Freundlich	$q = KC^{1/n}$	(2)		
n			1.89	0.90
K			0.00817	
Halsey	$\ln q = [(1/n)\ln K] - (1/n)\ln[\ln(1/C)]$	(3)		
n			0.163	0.91
K			0.515	
Henderson	$\ln q = (1/n)\ln[\ln(1-C)] - (1/n)\ln K$	(4)		
n			1.89	0.91
K			8690.5	
Smith	$q = W_b - W\ln(1-C)$	(5)		
W			0.9327	0.90
W_b			6×10^{-6}	
D–R	$\ln q = \ln q_m - K_1\varepsilon^2$	(6)		
q_m	$[\varepsilon = RT\ln(1 + 1/C)]$		3.836×10^{-4}	0.90
K			4×10^{-9}	
E	$E = (2K_1)^{-0.5}$	(7)	11.18	

3.7. Thermodynamic analysis

Thermodynamic parameters can be calculated using the following equations [20]. The distribution constant can be written as:

$$k_D = \frac{C_{ads}}{C_{non-ads}}. \quad (8)$$

The well known Gibbs free energy change can be expressed as:

$$\Delta G = -RT\ln k_D. \quad (9)$$

ΔG is related to the enthalpy and entropy change as follows:

$$\Delta G = \Delta H - T\Delta S. \quad (10)$$

The values of ΔG calculated using Eqs. (9) and (10) are given in Table 3. The plot of ΔG against T should give a straight line, as shown in Fig. 5. The values of ΔH and ΔS can be obtained from the intercept and the slope of the line, respectively. For this biosorption process, ΔH was found to be −68 542 J/mol, and ΔS to be −206.6 J/mol.

The negative values of ΔG show that the biosorption is a spontaneous process. The negative value of ΔH shows that the process has an exothermic character; therefore, increasing the temperature decreases the adsorption yield. The negative values of ΔS are due to the adsorbed ions that gain more ordered positions on the biosorbent surface compared to their situation in the solution.

3.8. Adsorption kinetics

An adsorption rate expression is necessary in order to design a fast and effective process [21]. Several models can be used to

Table 3
Values of ΔG at different temperatures.

Temperature (K)	283	293	303	313
ΔG (J/mol)	−9181	−8489	−6775	−2866

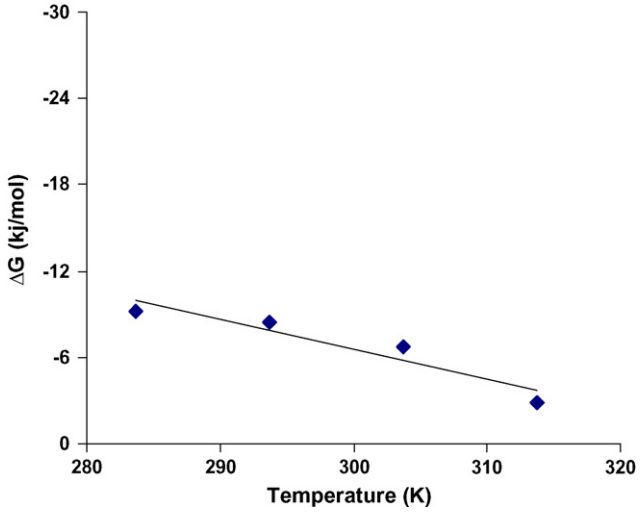

Fig. 5. Plot of ΔG vs. T.

express the mechanism of solute sorption onto a sorbent. Adsorption is a physiochemical process that involves the mass transfer of a solute from the fluid phase to the adsorbent surface. The study of adsorption kinetics describes the solute uptake rate. In order to examine the controlling mechanisms of the adsorption process, such as the chemical reaction, intra-pore diffusion, and mass transfer through fluid film, several kinetic models are used to test the experimental data. From a system design point of view, the analysis of adsorption rates using different kinetic equations is important for practical operations [22–23].

In the present work, the parameters, which have considerable effects on the biosorption, were the initial pH of the solution and biosorption dose. The effect of the pH can be explained by the difference between the electrical charge of the adsorbed species and the surface charge: that is, the electrical force. The temperature, particle size, and stirring speed were less effective on the process. The important effect of the particle size shows that the diffusion of Ga-67 through the pores in the biosorbent may be an important step in controlling the rate of the biosorption process. The small effect of the stirring speed indicates that the diffusion through the film layer around the biosorbent particle is not a controlling step. Therefore, the process may not be controlled by only one of the mechanisms of diffusion through the film layer, surface sorption, or diffusion through the pores; the mechanism that governs the process can probably be a combination of all these mechanisms. However, after the kinetic models were examined, it was determined that the biosorption fitted the pseudo-second order kinetic model. For an adsorption process, which fits the pseudo-second order kinetic model, the integrated equation can be given as follows [20,24]:

$$\left(\frac{t}{q_t}\right) = \frac{1}{(kq_e^2)} + \left(\frac{1}{q_e}\right) t \tag{11}$$

$$h = kq_e^2 \tag{12}$$

where h is the initial adsorption rate. The plot of t against t/q_t should give a straight line if the process fits the pseudo-second order rate model. The experimental data showed an excellent agreement with this kinetic model as shown in Fig. 6(a) for different pH values and in Fig. 6(b) for different temperatures. Table 4 also shows the excellent agreement between the experimental and calculated values. The R^2 values for the fit of the data to the kinetic model are very high, which are between 0.98 and 1.0.

The increase of the biosorption yield with the increase in the negative surface charge of prina and the decrease in temperature can also prove that the biosorption is of mainly physical character. The activation energy value for the process can show if the process is governed by a physical or chemical mechanism. The Arrhenius

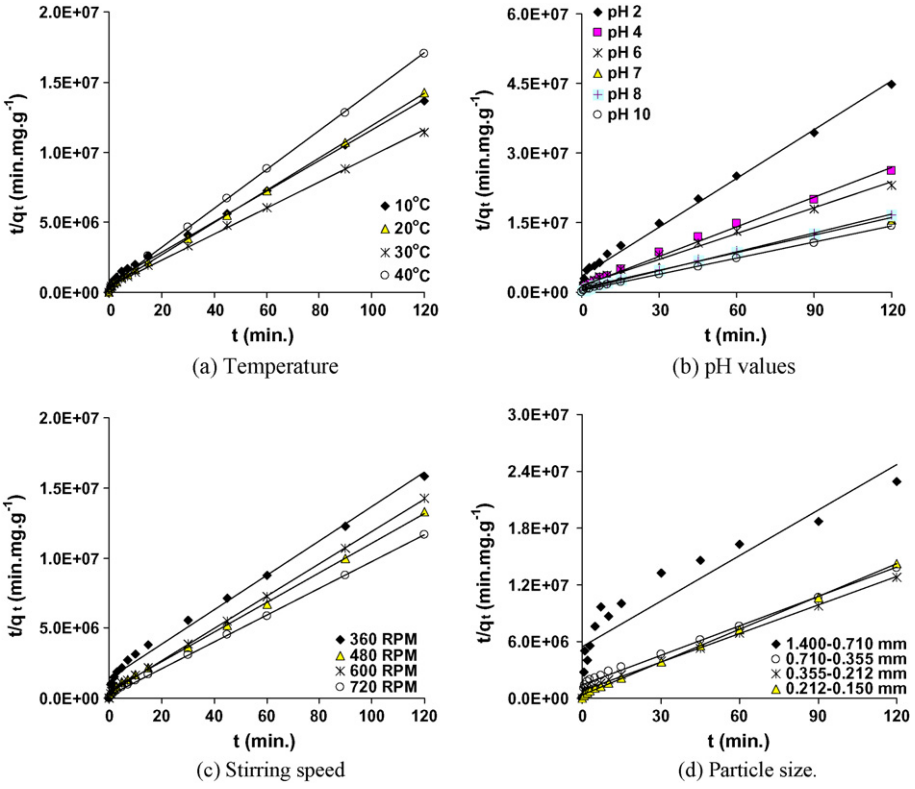

Fig. 6. Agreement of experimental data with pseudo-second order kinetic model. (a) Temperature; (b) pH values; (c) stirring speed; (d) particle size.

Table 4
Fit of experimental data with pseudo-second order kinetic model for experimental parameters.

Parameters	$q \times 10^6$ (mg g^{-1})	k (mg g^{-1} min^{-1})	$h \times 10^6$ (mg g^{-1} min^{-1})	R^2	$q(thr) \times 10^6$ (mg g^{-1})
Temperature (°C)					
10	8.8	18,174.6	1.5171	0.996	9.1364
20	8.42	36,558.5	2.7523	0.999	8.6767
30	10.483	21,639	2.4844	0.998	10.715
40	7.035	49,056.6	2.5345	0.999	7.1879
pH					
2	2.673	41,058.4	0.3334	0.990	2.8493
4	4.577	45,690.3	1	0.994	4.6783
6	5.225	34,484.9	1	0.989	5.385
7	7.73	18,313.7	1.1368	0.989	7.879
8	7.177	34,656.2	1.8926	0.998	7.390
10	8.42	36,558.5	2.7523	0.999	8.6767
Stirring speed (rpm)					
360	7.567	15,116.2	1	0.988	8.1335
480	9.033	23,710.4	2.1099	0.999	9.4334
600	8.42	36,558.5	2.7523	0.999	8.6767
720	10.27	43,416.2	4.7566	0.999	10.467
Particle size (mm)					
1.400–0.710	5.234	5,123	0.2	0.859	6.2482
0.710–0.355	8.686	10,849.3	1	0.987	9.6006
0.355–0.212	9.39	13,344.8	1.3098	0.996	9.9071
0.212–0.150	8.42	36,558.5	2.7523	0.999	8.6767

equation is expressed in the following form:

$$k = A\, e^{-E_a/RT} \tag{13}$$

$$\ln k = \ln A - \frac{E_a}{R}\frac{1}{T} \tag{14}$$

The activation energy can be calculated graphically from the plot of ln k against $1/T$, as shown in Fig. 7. The activation energy was calculated to be 18.105 kJ/mol; this low value confirms that the process is not governed by the surface chemical reaction. This value lies in the range of 8–22 kJ/mol K for the diffusion-controlled process [20,24]. However, it is still thought that the process is not governed by the diffusion through the film layer around the particle since no effect of the stirring speed was observed.

In conclusion, for the biosorption mechanism, the Freundlich, Halsey, Henderson, and Smith isotherm regression coefficient values (R^2) > 0.9 imply that the surface of prina is made up of heterogeneous and multilayered biosorption patches. All of the studied ranges, the standard Gibbs free energy (ΔG) values, and the ΔH parameter were found to be negative and indicated the thermodynamically feasible, spontaneous, and exothermic nature of the biosorption. The negative ΔS value implies a stable arrangement of gallium on the prina biomass surface and that the adsorbed complex of gallium on prina is in a more ordered form [25,26].

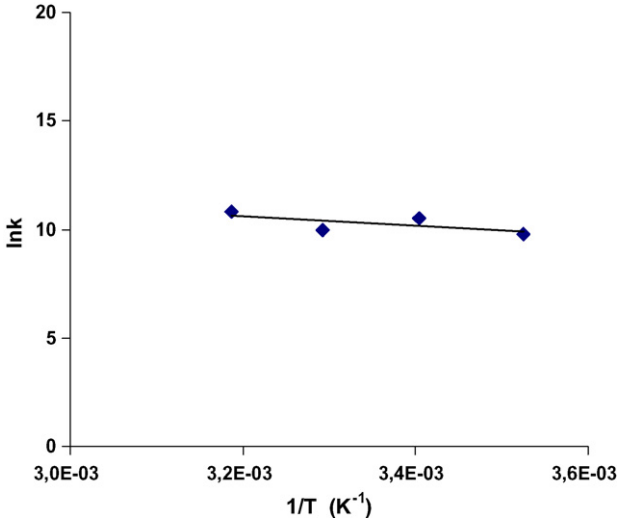

Fig. 7. Plot of ln K vs. $1/T$.

3.9. Adsorption mechanism of Ga-67 adsorbed in prina

Generally, there are three consecutive main transition steps in any adsorption process. These are film diffusion, intraparticle or pore diffusion, and sorption to inside regions. In adsorption, the last one can be ignored since it is the fastest one among the three steps. The slower of the film diffusion step and the pore diffusion step can be declared as the one that controls the process [22]. According to Weber and Morris [27], if the controlling step of adsorption is the intraparticle step, then the adsorbent of q_t varies with the square root of the adsorption period. Hence, the adsorption rate is measured as a function of the square root of time by determining the absorption capacity of the absorbent. The Weber and Morris equation is given as follows [27]:

$$q_t = k_i\sqrt{t} + Z. \tag{15}$$

The diffusion coefficient depends heavily on surface properties of the absorbent. The diffusion coefficient for adsorption can be calculated as follows [28,29]:

$$f\left(\frac{q_t}{q_e}\right) = -\log\left[1 - \left(\frac{q_t}{q_e}\right)\right] = \frac{\pi^2 Dt}{2.3r_o^2}. \tag{16}$$

By taking the pseudo-second order model into consideration [27]:

$$t_{1/2} = \frac{1}{k \cdot q_e}. \tag{17}$$

If calculated by placing the halving time into the equation, $t_{1/2}$ is found as:

$$t_{1/2} = \frac{0.030 r_0^2}{D}. \tag{18}$$

Graphs related to intraparticle diffusion are analyzed, and it is observed that the graphs fit the mechanism (Table 5 and Fig. 8). And related calculations are shown in Table 5.

When graphs related to intraparticle diffusion are analyzed, it is seen that the regression coefficients are high, which leads to the

Table 5
The calculations of intraparticle model.

Parameters	$t_{1/2}$ (min)	$k_i \times 10^8$ (mg/g s$^{0.5}$)	$D \times 10^{13}$ (m^2/s)	R^2
Temperature (°C)				
10	6.25	10	6.550	0.904
20	3.25	8	12.606	0.788
30	4.41	10	9.289	0.845
40	2.90	6	14.133	0.802
pH				
2	9.11	3	4.494	0.937
4	5.90	5	8.564	0.903
6	8.10	6	7.379	0.954
7	7.07	8	5.797	0.965
8	4.03	7	10.186	0.852
10	3.24	8	12.606	0.788

conclusion that adsorption is a result of either pore diffusion or intraparticle diffusion. Looking at the data, the shortening of the adsorption time with increases in temperature and the pH level, as supported by other analysis results, strengthens the belief of physical adsorption. The increase in the diffusion coefficient with the increase in temperature is already expected. Since increased diffusion with the increase in temperature results in the increased activity of the metal to be adsorbed, the increase in the amount of the material that can hold on to the surface of the metal supports the event described. Again, the increase in the pH and diffusion coefficients shows that diffusion can occur more easily. This belief is supported by the increase in the adsorption efficiency with the increase in the pH in this study. Aggravated ionized power with the increasing negativeness of surface loads increases diffusion, and as a result of this, the adsorption efficiency gets higher. Here k_i decreases with temperature whereas it increases with the pH. Taking all of this into account, we can see that either pore or intraparticle diffusion is realized all around the surface.

3.10. The FTIR and EPR results

In order to determine the main functional groups of WPOOF participate in Ga-67 radionuclide adsorption, it has recorded the natural and Cr(VI) loaded WPOOF. The FTIR spectra before and after adsorption are shown in Fig. 9.

Compared with the FTIR spectra before and after adsorption, there were clear band shifts and intensity decrease at fifteen bands. These bands are the functional groups of WPOOF participate in Ga-67 biosorption which are shown in Table 6.

For the determination of the functional groups acting in biosorption, the FTIR spectra of the adsorbents were taken before and after adsorption. The decaying FTIR spectrum corresponding to a certain group is an indication that the group played a role in the adsorption.

Table 6
FTIR spectral characteristics of WPOOF before and after adsorption.

IR peak	Frequency (cm^{-1})			Assignment
	Before ads.	After ads.	Differences	
1	3568	3604	−36	Bonded –OH groups
2	3511	3513	+2	Bonded –OH groups
3	3438	3438	0	Bonded –OH groups
4	3323	3286	−37	–NH_2 and –OH groups stretching
5	3188	3188	0	N–H stretching
6	2928	2927	−1	Aliphatic C–H group
7	1735	1728	−7	C=O stretching
8	1654	1661	+7	C=O stretching
9	1627	1627	0	C=O stretching
10	1595	1562	−33	Secondary amine group
11	1516	1508	−8	Secondary amine group
12	1455	1446	−9	Symmetric bending of CH_3
13	1420	1410	−10	Symmetric bending of CH_3
14	1378	1368	−10	Symmetric bending of CH_3
15	1317	1316	−1	Symmetric bending of CH_3
16	1268	1260	−8	–SO_3 stretching
17	1160	1155	−5	C–O stretching of ether groups
18	1048	1045	−3	C=O stretching
19	893	893	0	Aromatic –CH stretching
20	812	812	0	Aromatic –CH stretching
21	779	778	−1	Aromatic –CH stretching
22	672	668	−4	–CN stretching
23	558	550	−8	–C–C– group
24	456	446	−10	Amine groups
25	431	Unappeared	Unknown	Amine groups

The comparison of the spectra taken before and after adsorption shows that two spectra are very similar. However, the magnitudes of the peaks belonging to OH and NH_2 groups at 3568, 3323 and 1595 cm^{-1} diminish. This change is an indication that oxygen and nitrogen atoms containing electron couple interacts with radionuclide Ga by forming complexes [25–30].

Electron paramagnetic resonance (EPR) can be applied to the investigation of metal-charged biomasses. For this aim, the main information provided by this technique are the chemical identity, valence states and relative concentration of the metals involved in the biosorption processes [31]. In the early researches, the adsorption data were combined with EPR spectroscopy to obtain structural information about the metal binding and estimate of adsorption mechanism [32–36]. In order to investigate the natural and Ga-67 loading WPOOF and estimate Ga-67 ion biosorption mechanism, the EPR spectra were taken from the alone and Ga-67 loading biosorbent. The EPR spectra before and after adsorption of WPOOF are shown in Fig. 10.

It was shown in this figure that these spectra are two typical EPR signals belonging to Mn^{2+} and Fe^{3+} ion spectra. The biosorption of gallium by WPOOF is investigated by using Mn^{2+} and Fe^{3+} ion spectra. With $S = 5/2$(in the high spin case), $I = 5/2$ for Mn^{2+} with

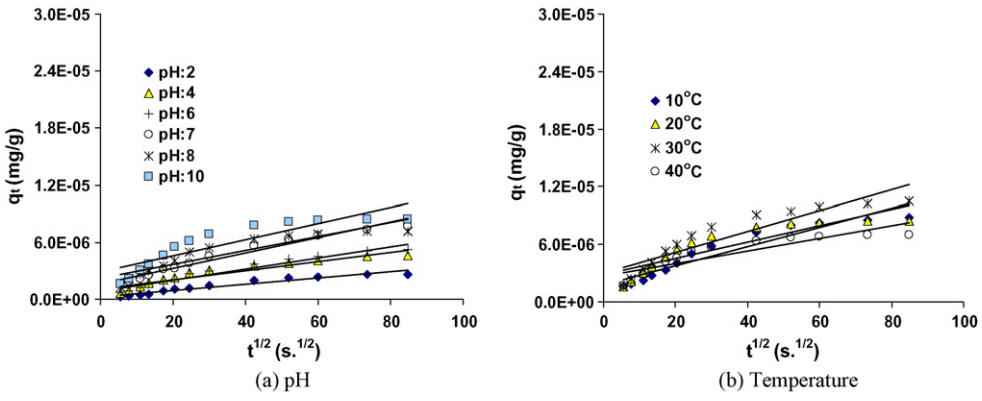

Fig. 8. Plots of q_t vs. $t_{1/2}$ for different pH (a) and temperature values (b).

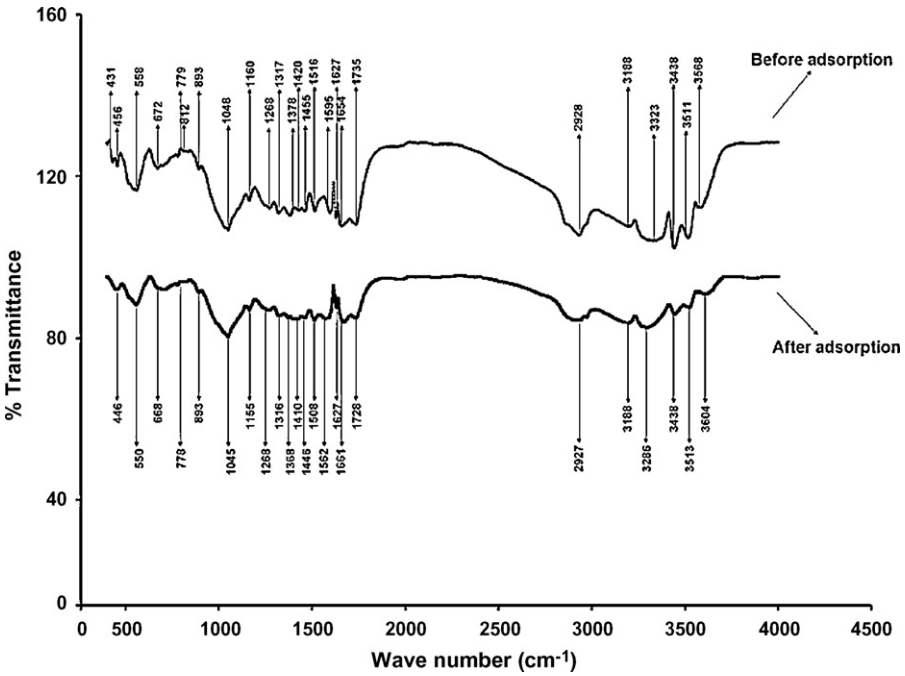

Fig. 9. FTIR spectra of WPOOF before and after adsorption.

100% natural abundance, g-Factor was calculated from resonance conditions as follows:

$$g = \frac{h\nu}{\beta B_r} \tag{19}$$

The seven lines were observed in these resonance absorption curves in Fig. 10. The broad EPR lines stem from strong dipolar interactions of their unpaired magnetic moments. It can be seen from this figure, the amplitude of some EPR signal decreased and some of them increased after adsorption. While the bands centered at 3056 G (g = 2.229), 3132.5 G (g = 2.170), 3256 G (g = 2.092) were decreased and disappeared, the amplitude of free radical band centered at 3400 G (g = 2.003) was increased after biosorption. The band centered at 3400 G (g = 2.003) belonging to Fe^{3+} free radicals and the amplitude of it enlarge as about two times. This occurrence indicated that the Fe^{3+} free radical intensities increase after adsorption. The other EPR bands belonging to Mn^{2+} ion spectra and all of them were lost after adsorption. These occurrences indicate that the Ga-67 radionuclide can be coordinating with the active sites of the adsorbent causing the pairing of the electrons. The g-value of free radical close to 2 confirms that the free-radical is an organic free-radical and the fast biosorption kinetics observed is typical for biosorption of metals involving no energy-mediated reactions, where metal removal from solution is due to physicochemical interactions between biomass and metal solution [37,38].

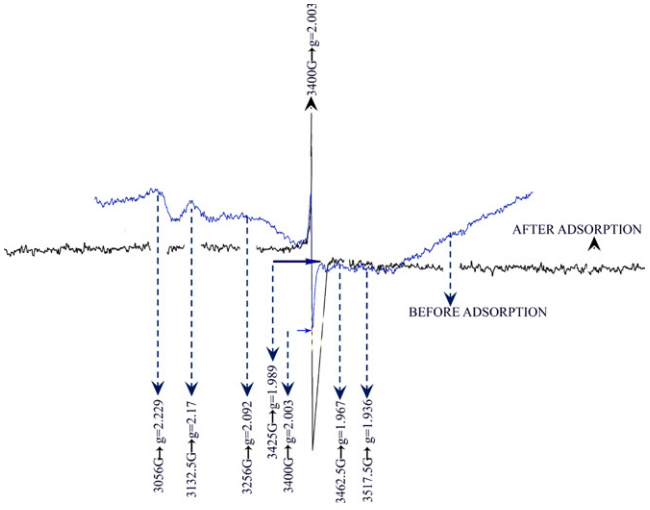

Fig. 10. EPR spectra for the natural and gallium loaded WPOOF were measured at room temperature (25 ± 2 °C) with a microwave frequency of 9.53 GHz.

4. Conclusion

In this study, Ga-67 radionuclides were adsorbed from liquid wastes by using a biosorbent. Prina was used as the biosorbent and the following results were obtained:

- Prina had very promising results as an adsorbent. Adsorption was stabilized in 120 min and the adsorption rate was high.
- The most effective parameters were the pH, temperature, the particle size, and the adsorbent ratio. It was also determined that the stirring speed did not have much effect on the adsorption.
- Ideal adsorption conditions were determined as 600 rpm stirring speed, 0.150–0.212 mm particle size, 20 °C temperature, 10 pH, and 10 g/L solid/fluid rate. Low stirring speed and low temperature values can be preferred due to economic reasons.
- In ideal adsorption conditions, the initial radioactive concentration was chosen as 500 μCi, and 97% of Ga-67 was adsorbed.
- Adsorption is characterized as exothermic, multilayered, heterogeneous, and physical.
- The experimental data exhibited a good agreement with the isotherm models of Freundlich, Halsey, Henderson, D–R, and Smith.
- Standard free Gibbs energy (ΔG) and ΔH parameters were taken into account, and bioadsorption is believed to have exothermic character and to be natural.
- The kinetics of adsorption was seen to fit a pseudo-second order reaction model.

- The mechanism of adsorption was believed to be either pore diffusion or intraparticle diffusion.

The Turkish government has ruled that the limit for Ga-67 is 1 μCi with the sixth and ninth provisions of the regulation numbered 15.01.2000/23934 that relate to radioactive materials that do not require special processes and with the tenth provision of the third section of the regulation that regulates the restrictions and limitations on dumping radioactive materials to the environment. Businesses are required to follow these provisions, and they are watched very closely.

Considering that the average weekly usage of Ga-67 in nuclear medical centers in Turkey is 8000–24,000 μCi, we can easily estimate that it is necessary to wait around 10–22 weeks before dumping the radioactive waste of even one week of usage to the environment. These types of establishments have weekly accumulated wastes, and since the method of having the wastes in lead tanks is both expensive and slow, this method is difficult to apply if the regulation code is followed. Furthermore, since Ga-67 turns into Zn-67 and becomes hazardous pollutants in this form, it is clear that they cannot be dumped in the environment. The following proposals can be considered:

- Removing radioactive materials using adsorption is believed to protect the environment from harmful effects of radiation.
- Since a radioactive material also turns into a harmful metal in stable states, additional protection from this harmful effect is needed.
- Elimination of this heavy metal or its radioactive state, which is dumped to the environment, by using adsorbents or storing in lead tanks, seems economically not possible. It is clearly seen that 80% of Ga-67 in 1 m^3 of liquid waste can be adsorbed by using 1.5 kg of an adsorbent.
- Optimum conditions can be established by analyzing this absorbent among other adsorbents.
- It is believed that important economical benefits will be gained since the adsorbent, which is a waste matter itself, and the materials it adsorbs will not be dumped to the environment in their harmful form and they can be recycled with further suitable processes.
- More effective and suitable projects can be generated for radiation research centers or establishments.

Acknowledgement

The support of Atatürk University for the project BAP-2003/372 is highly appreciated.

References

[1] J.G. Dean, F.L. Bosqui, K.H. Lanoutte, Removing heavy metals from waste waters, Environ. Sci. Technol. 6 (1972) 518–524.
[2] B. Volesky, Biosorption and Biosorbents, Biosorption of Heavy Metals, CRP Press, Boca Raton, FL, Florida, 1990.
[3] A. Görpe, S. Cantez, Pratik Nükleer Tıp, İstanbul Tıp Fakültesi Vakfı, İstanbul (1992).
[4] E.İ. Medine, Hasta İyonunun I-131′in Amberlit Anyon Değiştirici Reçine ile Tutulması, Ege Üniversitesi Fen Bilimleri Enstitüsü, Turkey, 2003.
[5] H. Koshima, Adsorbtion of iron(III), gold(III), gallium(III), thallium(III) and antimony(V) on Amberlite XAD and Chelex 100 resins from hydrochloric acid solution, Anal. Sci. 2 (1986) 225–260.
[6] S.T. Taner, Z. Demirel, Z. Üst, Medikal Alanda Ortaya Çıkan Cr-51 Atıkları için Kullanilabilecek Biyolojik Kökenli Bir Adsorban Teklifi, Ege Üniversitesi Fen Bilimleri Enstitüsü, Turkey, 2003.
[7] C. Kütahyalı, Mangal Kömüründen Üretilen Aktif Karbon Kullanılarak Uranyumun Selektif Adsorpsiyonunun ve Uygulama Alanlarının İncelenmesi, Ege Üniversitesi Fen Bilimleri Enstitüsü, Turkey, 2002.
[8] P.K. Sinha, K.B. Lal, J. Ahmed, Removal of radioiodine from liquid effluents, Pergamon, Waste Manage. 17 (1997) 33–37.
[9] A.E. Osmanlioglu, Treatment of radioactive liquid waste by sorption on natural zeolite in Turkey, J. Hazard. Mater. B137 (2006) 332–335.
[10] R.J. Kowalsky, J.R. Perry, Radiopharmaceuticals in Nuclear Medicine Practice, Appleton & Lange, California, 1987.
[11] G.B. Saha, Fundamentals of Nuclear Pharmacy, Springer-Verlag, New York, 1984.
[12] E. Kurtuluş, Prina kurutulması ve prinanın yakıt olarak kullanılmasının araştırılması, Ege Ünv., Fen Bil. Ens., Makina Müh. Anabilim Dalı, Turkey, 2004.
[13] C.R. Bansal, M. Goyal, Activated Carbon Adsorption, Taylor and Francis Group, United States of America, 2005, pp. 85–93.
[14] H.Y. Erbil, Surface Chemistry of Solid and Liquid Interfaces, Blackwell Publishing, Gebze Institute of Technology, Turkey, 2006, pp. 300–302.
[15] T. Shek, A. Ma, V.K.C. Lee, G. McKay, Kinetics of zinc ions removal from effluents using ion exchange resin, Chem. Eng. J. 146 (2009) 63–70.
[16] J.U.K. Oubagaranadin, N. Sathyamurthy, Z.V.P. Murthy, Evaluation of Fuller's earth for the adsorption of mercury from aqueous solutions: a comparative study with activated carbon, J. Hazard. Mater. 142 (2007) 165–174.
[17] H.M. Jnr, A.I. Spiff, Equilibrium sorption study of Al^{3+}, Co^{2+} and Ag^{+} in aqueous solutions by fluted pumpkin (Telfairia Occidentalis HOOK f) waste biomass, Acta Chim. Slov. 52 (2005) 174–181.
[18] E. Oguz, B. Keskinler, Determination of adsorbtion capacity and thermodynamic parameters of the PAC used for Bomaplex Red CR-L dye removal, Colloids Surf. A 268 (2005) 124–130.
[19] P. Antonio, K. Iha, M.E.V. Suárez-Iha, Adsorption of di-2-pyridyl ketone salicyloylhydrazone on silica gel: characteristics and isotherms, Talanta 64 (2004) 484–490.
[20] J. Febriantoa, A.N. Kosasiha, J. Sunarsob, Y.H. Jua, N. Indraswati, S. Ismadjia, Equilibrium and kinetic studies in adsorption of heavy metals using biosorbent: a summary of recent studies, J. Hazard. Mater. 162 (2009) 616–645.
[21] M. Arami, N.Y. Limaee, N.M. Mahmoodia, Evaluation of the adsorption kinetics and equilibrium for the potential removal of acid dyes using a biosorbent, Chem. Eng. J. 139 (2008) 2–10.
[22] M. Alkan, M. Doğan, Y. Turhan, Ö. Demirbaş, P. Turan, Adsorbtion kinetics and mechanism of maxilon blue 5G dye on sepiolite from aqueous solutions, Chem. Eng. J. 139 (2008) 213–223.
[23] I.A.W. Tan, A.L. Ahmad, B.H. Hameed, Adsorption isotherms, kinetics, thermodynamics and desorption studies of 2,4,6-trichlorophenol on oil palm empty fruit bunch-based activated carbon, J. Hazard. Mater. 164 (2009) 473–482.
[24] H. Eroğlu, S. Yapici, Ç. Nuhoğlu, E. Varoğlu, An environmentally friendly process: adsorption of radionuclide Tl-201 on fibrous waste tea, J. Hazard. Mater. 163 (2009) 607–617.
[25] E. Malkoc, Y. Nuhoglu, Potantial of tea factory waste for chromium(VI) removal from aqueous solutions: thermodynamic and kinetic studies, Sep. Purif. Technol. 54 (2007) 291–298.
[26] S.P. Dubey, K. Gopal, Application of natural adsorbent from silver impregnated *Arachis hypogaea* based thereon in the processes of hexavalent chromium for the purification of water, J. Hazard. Mater. 164 (2009) 968–975.
[27] W.J. Weber, J.C. Morris, J. Sanit, Kinetics of adsorbtion on carbon from solution, Eng. Div. 89 (1963) 31–59.
[28] D. Kavitha, C. Namasivayam, Experimental and kinetic studies on methylene blue adsorbtion by coir pith carbon, Bioresour. Technol. 98 (2007) 14–21.
[29] G. Crini, H.N. Peindy, F. Gimbert, C. Robert, Removal of C.I. Basic Green 4 (Malachite Green) from aqueous solutions by adsorption using cyclodextrin-based adsorbent: kinetic and equilibrium studies, Sep. Purif. Technol. 53 (2007) 97–110.
[30] H. Lata, V.K. Garg, R.K. Gupta, Sequestration of nickel from aqueous solution onto activated carbon prepared from *Parthenium hysterophorus* L., J. Hazard. Mater. 157 (2008) 503–509.
[31] R.P. De Carvalho, J.R. Freitas, A.M.G. De Sousa, R.L. Moreira, M.V.B. Pinheiro, K. Krambrock, Biosorption of copper ions by dried leaves: chemical bonds and site symmetry, Hydrometallurgy 71 (2003) 277–283.
[32] R.P. De Carvalho, K.J. Guedes, M.V.B. Pinheiro, K. Krambrock, Biosorption of copper by dried plant leaves studied by electron paramagnetic resonance and infrared spectroscopy, Hydrometallurgy 59 (2001) 407–412.
[33] P. Merdy, E. Guillon, M. Aplincourt, J. Dumonceau, H. Vezin, Copper sorption on a straw lignin: experiments and EPR characterization, J. Colloid Interf. Sci. 245 (2002) 24–31.
[34] K. Flogeac, E. Guillon, M. Aplincourt, Adsorption of several metal ions onto a model soil sample: equilibrium and EPR studies, J. Colloid Interf. Sci. 286 (2005) 596–601.
[35] S. Sayen, F. Chuburu, E. Guillon, M. Aplincourt, H. Handel, M. Le Bacon, V. Patinec, Copper sorption onto a lignocellulosic substrate from wheat bran impregnated with a lipophilic tetraazamacrocycle, Colloid Surf. A 289 (2006) 126–132.
[36] E. Buszman, B. Pilawa, M. Zdybel, S. Wilczynski, A. Gondzik, T. Witoszynska, T. Wilczok, EPR examination of Zn^{2+} and Cu^{2+} binding by pigmented soil fungi Cladosporium cladosporioides, Sci. Total Environ. 363 (2006) 195–205.
[37] I.P. Suhasini, G. Sriram, S.R. Asolekar, G.K. Sureshkumar, Biosorptive removal and recovery of cobalt from aqueous systems, Process Biochem. 34 (1999) 239–247.
[38] J.E. Wertz, J.R. Bolton, Electron spin resonance, Elementary Theory and Practical Applications, New York, 1972, p. 13.